Supplementary Information for: The Role of the Metal in Metal/MoS_2 and Metal/Ca_2N/MoS_2 Interfaces

Adrian F. Rumson,[1] Mohammad Rafiee Diznab,[2] Jesse Maassen,[2] and Erin R. Johnson[1,2]

[1)] *Department of Chemistry, Dalhousie University*

[2)] *Department of Physics & Atmospheric Science, Dalhousie University*

6 January 2025

Table S1: Computed properties of metal/MoS_2 heterostructures. N_{atoms} is the total number of atoms in the unit cell, while n_{MoS_2} is the number of MoS_2 formula units. Other quantities are defined in the main text of the article.

Interface	N_{atoms}	n_{MoS_2}	$\varepsilon_{\text{metal}}$ (%)	$\Delta\bar{z}_{S-\text{metal}}$ (Å)	ς_{Mo} (Å)	Q_{MoS_2} (e^-/MoS_2)	TBH (eV)	TBW (Å)	IGS (10^{14} e^-/cm^2)
Sb(0001)/MoS_2	81	13	−0.86	3.08±0.04	0.00	0.04	3.00	1.41	0.45
Sb(01$\bar{1}$2)/MoS_2	59	8	+0.68	3.07±0.08	0.00	0.06	3.02	1.33	1.43
Bi(0001)/MoS_2	111	19	+2.17	3.11±0.03	0.03	0.02	2.80	1.30	0.82
Bi(01$\bar{1}$2)/MoS_2	43	6	−0.99	3.05±0.06	0.00	0.08	2.64	1.17	1.28
Au/MoS_2	135	13	−2.10	2.70±0.05	0.00	0.02	1.88	0.97	1.76
Ag/MoS_2	162	16	−0.09	2.54±0.01	0.00	0.08	1.77	0.77	2.21
Cu/MoS_2	150	12	−0.26	2.26±0.06	0.01	0.12	0.72	0.42	2.70
Pt/MoS_2	33	3	−1.11	2.33±0.04	0.00	0.01	1.13	0.48	5.48
Ru/MoS_2	105	3	+0.76	2.22±0.01	0.01	0.14	-0.04	-	4.33
Y/MoS_2	30	4	+1.66	2.24±0.14	0.18	0.44	-1.21	-	6.19
W/MoS_2	73	8	+1.87	1.94±0.23	0.04	0.34	-3.22	-	6.70
Mo/MoS_2	130	13	+2.73	1.70±0.26	0.03	0.30	-3.79	-	5.92

Table S2: Computed properties of minimally strained metal/Ca_2N/MoS_2 heterostructures.

Interface	N_{atoms}	n_{MoS_2}	n_{Ca_2N}	$\varepsilon_{\text{metal}}$ (%)	ε_{Ca_2N} (%)	$E^{\text{strain}}_{\text{metal}}$ (meV/Å^2)	$E^{\text{strain}}_{Ca_2N}$ (meV/Å^2)	$E^{\text{unstr}}_{\text{exfol}}$ (meV/Å^2)	ς_{Mo} (Å)	$E^{MoS_2}_{\text{Gap}}$ (eV)	Q_{MoS_2} (e^-/MoS_2)
Au/Ca_2N/MoS_2	198	13	10	−2.10	+5.52	9.6	12.6	211.6	0.12	1.0	0.24
Ag/Ca_2N/MoS_2	201	16	14	−0.09	+2.35	0.0	2.7	223.1	0.15	0.7	0.30
Cu/Ca_2N/MoS_2	234	12	10	−0.26	+1.67	0.2	1.4	249.7	0.13	0.9	0.27
Ru/Ca_2N/MoS_2	159	12	10	+0.76	+1.67	3.8	1.4	263.6	0.12	0.9	0.25
W/Ca_2N/MoS_2	182	16	13	+1.87	+1.67	10.8	1.4	215.8	0.13	0.8	0.25
Mo/Ca_2N/MoS_2	301	25	19	+0.98	−1.01	3.2	0.5	220.9	0.14	0.7	0.29

Interface	MoS_2/Ca_2N			Ca_2N/metal		
	$\Delta\bar{z}$ (Å)	TBH (eV)	TBW (Å)	$\Delta\bar{z}$ (Å)	TBH (eV)	TBW (Å)
Au/Ca_2N/MoS_2	2.48±0.11	0.47	0.44	2.61±0.14	1.28	0.68
Ag/Ca_2N/MoS_2	2.44±0.10	-0.05	-	2.68±0.07	1.09	0.67
Cu/Ca_2N/MoS_2	2.50±0.11	0.40	0.40	2.62±0.05	1.42	0.75
Ru/Ca_2N/MoS_2	2.50±0.11	0.41	0.42	2.71±0.03	1.60	0.78
W/Ca_2N/MoS_2	2.46±0.11	0.28	0.32	2.69±0.06	0.83	0.59
Mo/Ca_2N/MoS_2	2.47±0.11	0.16	0.25	2.42±0.10	0.31	0.35

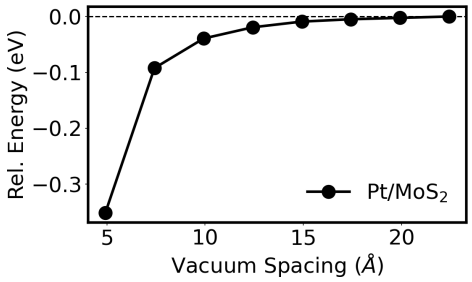

Figure S1: Convergence of the electronic energy with respect to the vacuum spacing for the Pt/MoS_2 heterostructure.

Table S3: Decomposed exfoliation energies of metal/MoS_2 heterostructures in meV/Å^2.

Interface	$E_{\text{exfol}}^{\text{str}}$	$E_{\text{exfol}}^{\text{str,PBE}}$	$E_{\text{exfol}}^{\text{str,XDM}}$	$E_{\text{metal}}^{\text{strain}}$	$E_{\text{exfol}}^{\text{unstr}}$
Sb(0001)/MoS_2	20.2	-0.3	20.4	0.9	19.3
Sb(01$\bar{1}$2)/MoS_2	28.1	-1.7	29.8	1.0	27.1
Bi(0001)/MoS_2	20.7	-2.8	23.5	2.2	18.6
Bi(01$\bar{1}$2)/MoS_2	28.5	-0.6	29.1	1.9	26.6
Au/MoS_2	33.9	-3.8	37.7	9.6	24.3
Ag/MoS_2	45.3	8.4	36.9	0.0	27.1
Cu/MoS_2	68.0	12.7	55.3	0.2	67.8
Pt/MoS_2	59.1	8.0	51.1	4.9	54.2
Ru/MoS_2	104.9	43.6	61.4	3.8	101.2
Y/MoS_2	101.0	66.0	35.1	3.1	98.0
W/MoS_2	122.2	74.7	47.6	10.8	111.4
Mo/MoS_2	89.2	22.5	66.7	24.2	65.0

Table S4: Computed properties of selected Ca_2N/MoS_2 heterostructures. n refers to the number of formula units of each component.

Property	Geom A	Geom B	Geom C	Geom D	Geom E
MoS_2 n	9	4	16	19	13
MoS_2 strain (%)	0.00	0.00	0.00	0.00	0.00
MoS_2 ς_{Mo} (Å)	0.04	0.19	0.13	0.14	0.15
MoS_2 E_{gap} (eV)	1.3	0.5	0.9	0.7	0.6
Ca_2N n	7	3	13	16	9
Ca_2N strain (%)	0.14	1.67	2.35	4.20	5.23
Ca_2N E_{strain} (meV/Å^2)	0.0	1.4	2.7	8.3	12.6
Q_{MoS_2} (e$^-$)	0.35	0.35	0.36	0.36	0.34
$E_{\text{exfol}}^{\text{str}}$ (meV/Å^2)	86.0	86.9	89.2	88.1	76.3
$E_{\text{exfol}}^{\text{unstr}}$ (meV/Å^2)	86.0	85.2	86.5	79.8	63.7

Table S5: Computed properties of metal/Ca_2N/MoS_2 heterostructures with the Ca_2N/MoS_2 bilayers constrained to either Geometry A or Geometry B.

Metal	Geometry	N_{atoms}	$\varepsilon_{\text{metal}}$ (%)	ς_{Mo} (Å)	$E_{\text{Gap}}^{\text{MoS}_2}$ (eV)
Au	A	120	4.14	0.04	1.4
Ag	A	120	6.05	0.04	1.4
Cu	A	126	4.69	0.04	1.4
Ru	A	126	3.29	0.04	1.5
W	A	120	5.90	0.03	1.4
Mo	A	100	6.67	0.03	1.5
Au	B	45	9.81	0.15	0.8
Ag	B	45	8.16	0.14	0.6
Cu	B	63	4.91	0.15	0.9
Ru	B	63	13.69	0.12	0.9
W	B	96	6.63	0.14	0.8
Mo	B	60	21.24	0.12	0.9

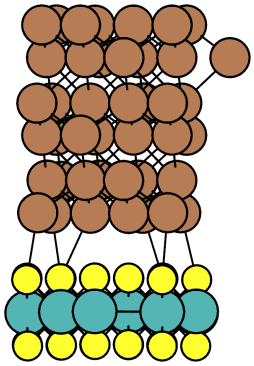

(a) Sb(0001)/MoS_2

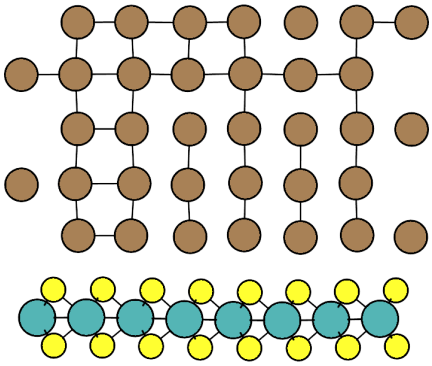

(b) Sb(01$\bar{1}$2)/MoS_2

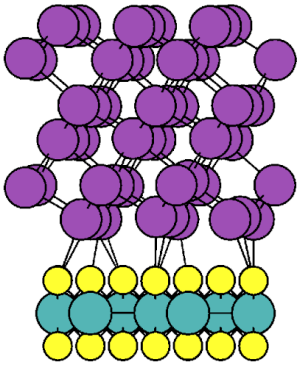

(c) Bi(0001)/MoS_2

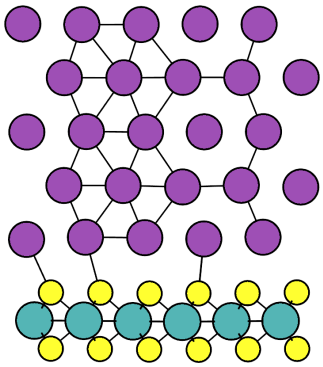

(d) Bi(01$\bar{1}$2)/MoS_2

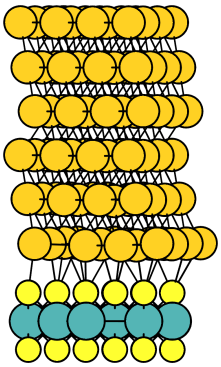

(e) Au/MoS_2

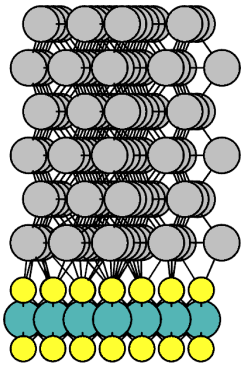

(f) Ag/MoS_2

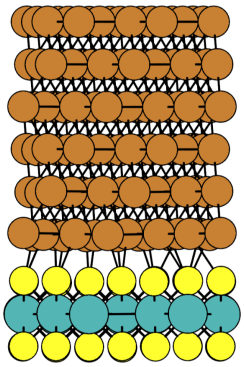

(g) Cu/MoS_2

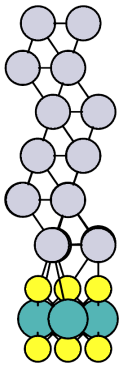

(h) Pt/MoS_2

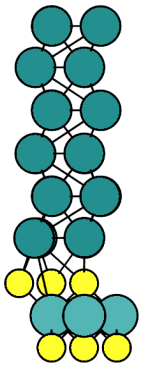

(i) Ru/MoS_2

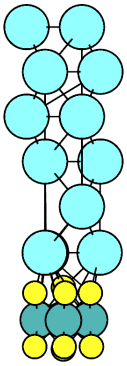

(j) Y/MoS_2

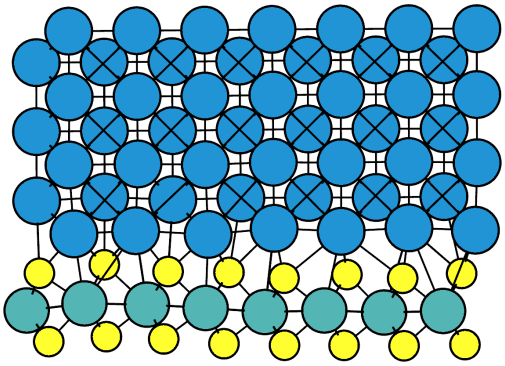

(k) W/MoS_2

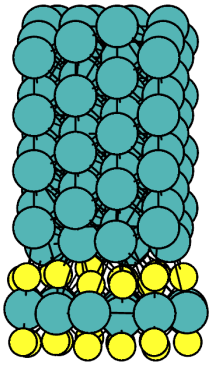

(l) Mo/MoS_2

Figure S2: Optimized geometries of metal/MoS_2 interfaces.

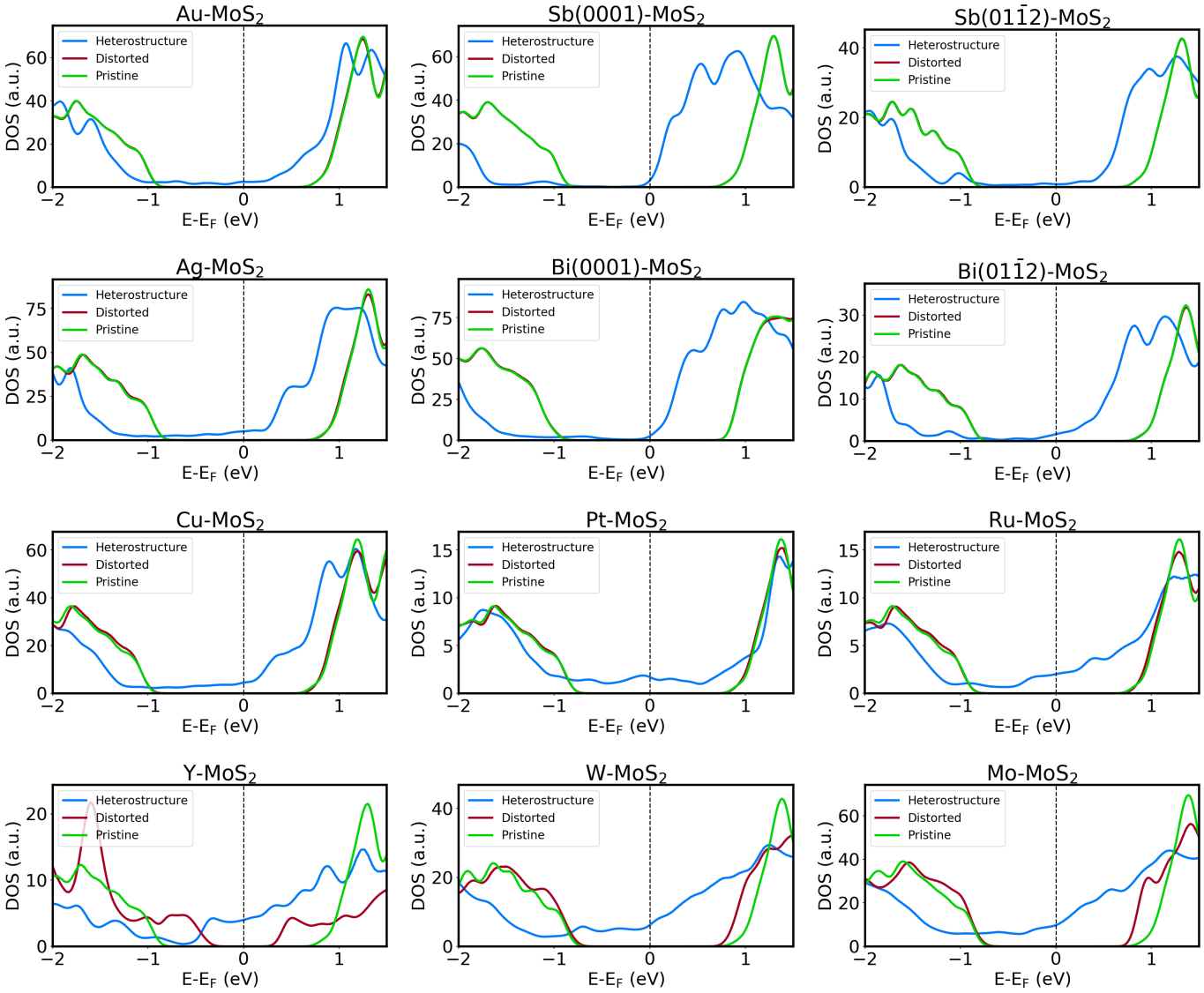

Figure S3: MoS_2 projected DOS for metal/MoS_2 interfaces.

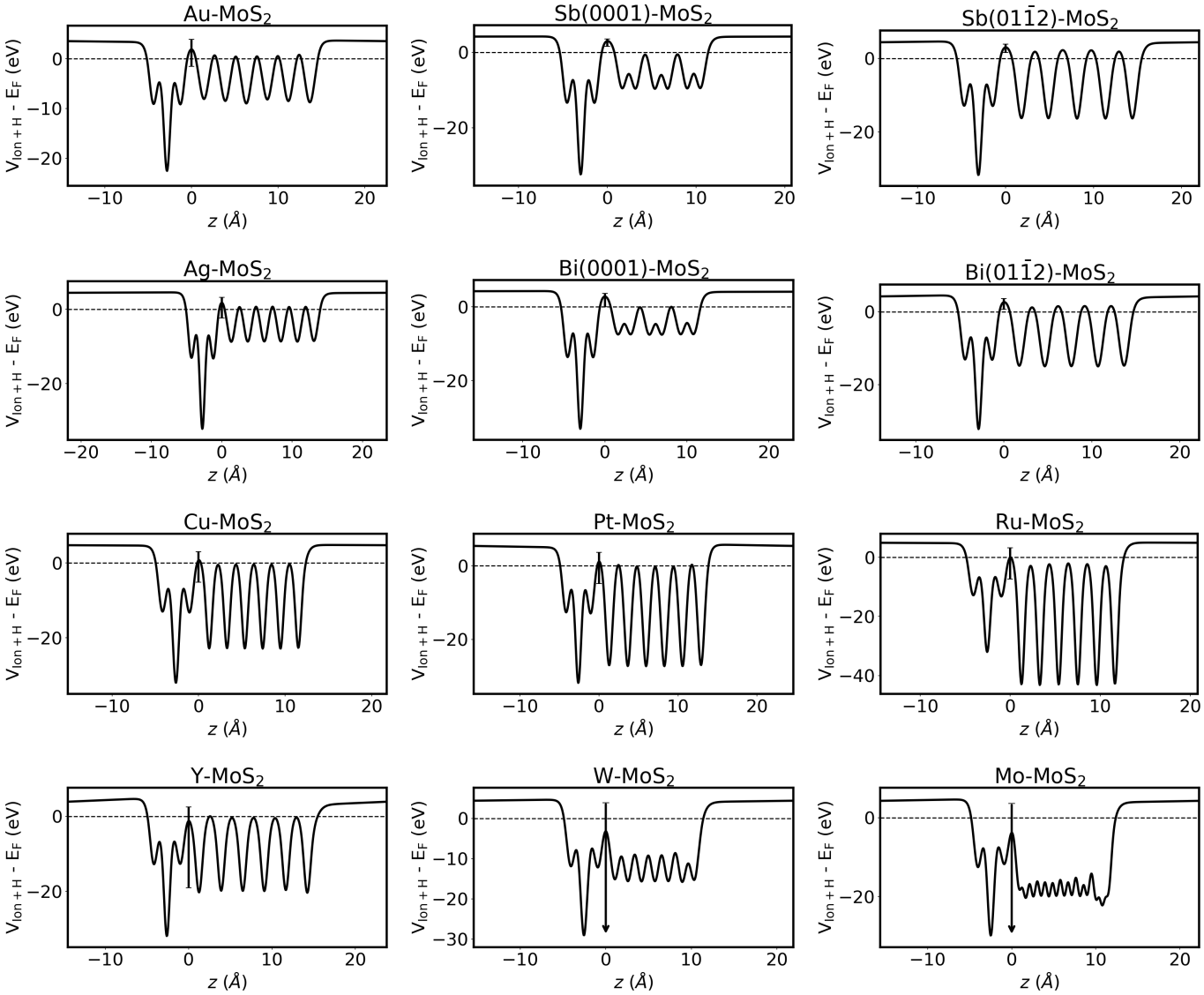

Figure S4: Averaged potential plots for metal/MoS_2 interfaces. The error bars indicate the maximum and minimum potential in the plane of the interface. For W and Mo, the arrow-error bars point to minimum potentials of -57.8 eV and -72.2 eV respectively.

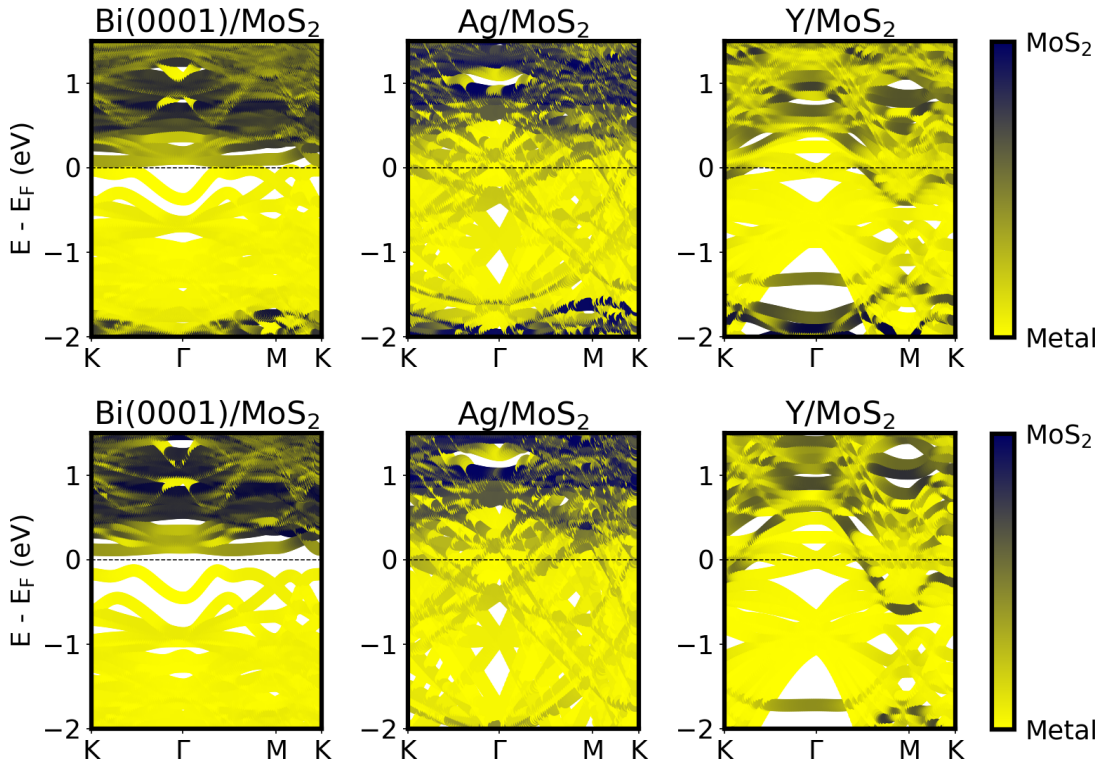

Figure S5: Kohn-Sham band structures computed using FHI-aims with PBE (top) or HSE06 (bottom) at the PBE-XDM QE-relaxed geometries. Three representative cases are shown: Bi(0001), (vdW), Ag (intermediate), and Y (covalent).

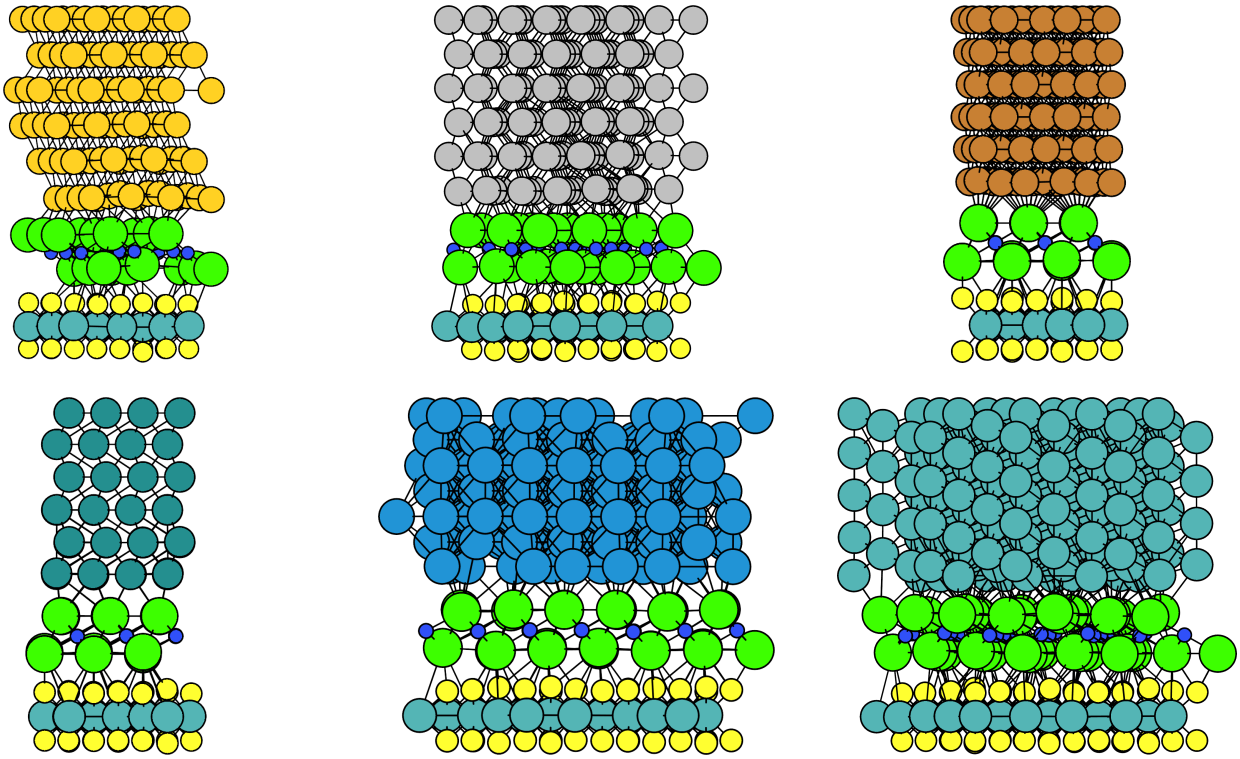

Figure S6: Optimized geometries of metal/Ca_2N/MoS_2 interfaces.

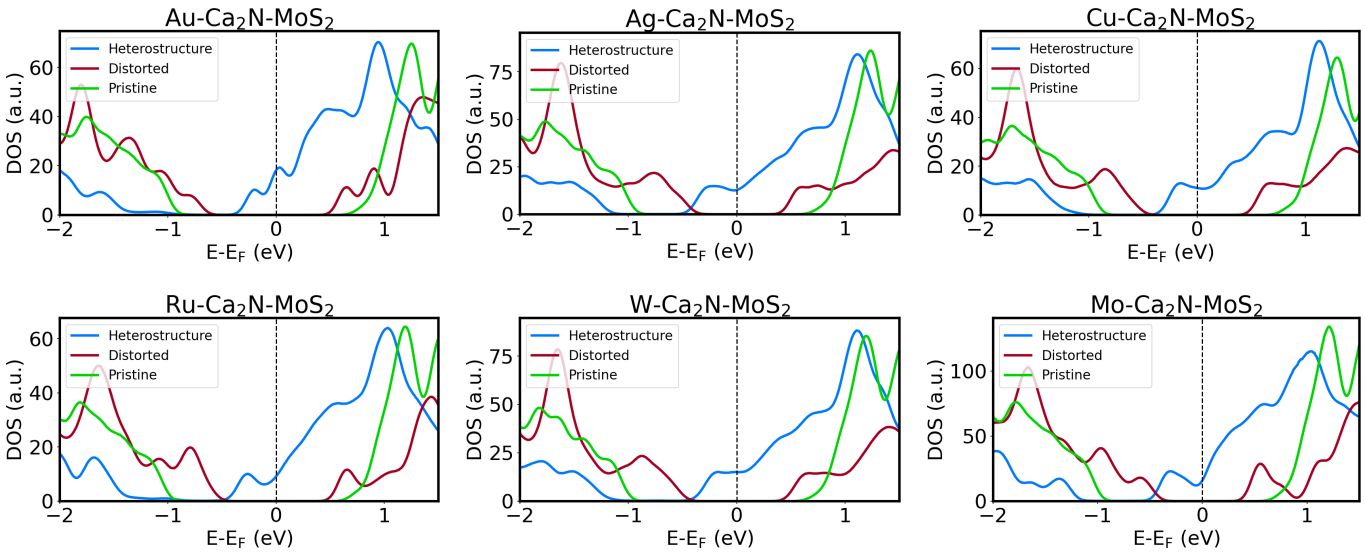

Figure S7: MoS_2 projected DOS for metal/Ca_2N/MoS_2 interfaces.

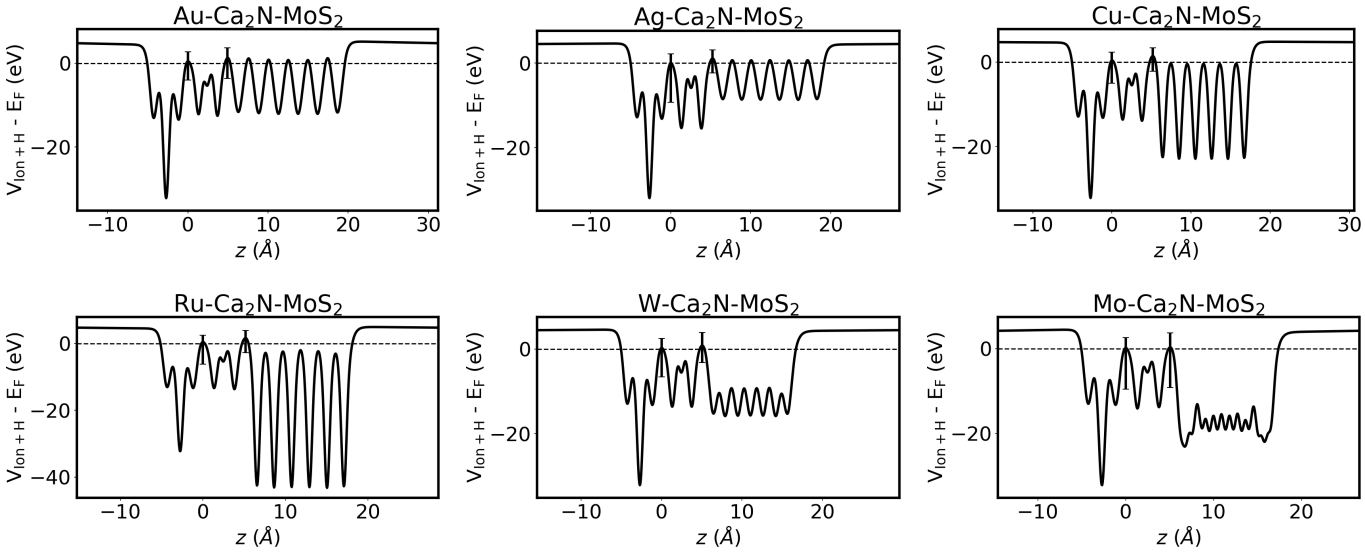

Figure S8: Averaged potential plots for metal/Ca_2N/MoS_2 interfaces. The error bars indicate the maximum and minimum potential in the plane of the interface.